



Optimal stimulated Raman adiabatic passage using the dynamical quantum geometric tensor

K. Z. Li , J. Z. Tian , and L. T. Xiao**Department of Physics, Taiyuan University of Technology, Taiyuan 030024, China* (Received 8 January 2024; revised 8 February 2024; accepted 15 February 2024; published 29 February 2024)

Stimulated Raman adiabatic passage is a prominent and widely applied technique that transfers population between quantum states in three-level quantum systems. In this paper, we propose an optimized version of stimulated Raman adiabatic passage, which can be implemented faster than the conventional version. In order to achieve quantum adiabaticity in shorter times, we use the geometric optimization method based on the dynamical quantum geometric tensor to regularize nonadiabatic transitions and to eliminate nonadiabatic effects during the evolution process. Optimal stimulated Raman adiabatic passage can shorten the operation time required for adiabatic population transfer appreciably, thereby avoiding decoherence resulting from long-time evolution. Moreover, optimal stimulated Raman adiabatic passage is robust against systematic and random errors. Our results provide an optimal route for the realization of fast and accurate population transfer in three-level quantum systems.

DOI: [10.1103/PhysRevA.109.022443](https://doi.org/10.1103/PhysRevA.109.022443)

I. INTRODUCTION

Precise control of the internal states in quantum systems leads to profound insights in atomic and molecular physics as well as novel applications, such as quantum information processing, quantum sensing, and metrology. As a fundamental task in quantum coherent control, accurate population transfer is often used for the preparation of given quantum states or the cooling of nanomechanical oscillators. Stimulated Raman adiabatic passage (STIRAP) [1–5] is a prominent and widely used technique for the realization of coherent population transfer between two dipole-forbidden or weakly coupled states in three-level quantum systems.

As a kind of quantum control technique based on adiabatic evolution, STIRAP is resilient against moderate variations of experimental parameters such as pulse amplitudes, duration, and single-photon detuning. Because of this advantage, STIRAP has been widely used in a variety of physical systems, like nitrogen-vacancy centers in diamond [6–10], superconducting circuits [11–13], semiconductor quantum dots [14–16], and optomechanics [17–20]. However, STIRAP requires the quantum system to evolve adiabatically. The speed of adiabatic evolutions is limited by the quantitative adiabatic condition [21–23], which can be generally expressed as

$$\left| \frac{\langle E_m(t) | \frac{\partial}{\partial t} | E_n(t) \rangle}{E_m(t) - E_n(t)} \right| \ll 1, \quad m \neq n, \quad t \in [0, \tau], \quad (1)$$

where $|E_n(t)\rangle$ are the entirely discrete and nondegenerate instantaneous eigenstates of Hamiltonian $H(t)$ with corresponding eigenvalues $E_n(t)$, and τ is the total evolution time. Therefore, STIRAP requires long evolution time to satisfy the quantitative adiabatic condition. This makes STIRAP vulnerable to environment-induced decoherence [5].

In order to realize fast population transfers, shortcuts to adiabaticity (STA) [24,25]—which include counterdiabatic driving, invariant-based inverse engineering, and fast-forward scaling approaches—have been used to speed up STIRAP [26–46] and design stimulated Raman exact passage [47–54]. However, although STA-based schemes mimic the adiabatic evolution in STIRAP, the robustness of STA-based schemes is not taken for granted. Indeed, a recent comparative study [55] on robust coherent control in three-level quantum systems showed that the STA-based schemes are sensitive to experimental errors, such as the Rabi frequency error and the detuning error, when compared to adiabatic population transfer.

Therefore, optimizing adiabatic processes in STIRAP to realize fast adiabatic population transfer is an important issue in the field of quantum control. Some efforts have been made on this issue, such as pulse shaping STIRAP [56] based on the Dykhne-Davis-Pechukas (DDP) method [57] and parallel STIRAP [58] by using detuning chirping. Although these protocols have been demonstrated to be effective in particular situations, they have some limitations. The DDP-based pulse shaping protocol is limited to the simple quantum systems that can be reduced to effective two-state systems. Parallel STIRAP requires controlling the detuning, which complicates experimental implementation. In this paper, we propose an optimized version of STIRAP by using the recently proposed geometric method [59] to speed up finite-time adiabatic processes. In contrast to the DDP method, the geometric method is applicable to general N -dimensional quantum systems. Thus, the optimal protocol for STIRAP based on the geometric method can be extended to more complicated quantum systems, such as the Heisenberg spin chain in which a STIRAP-like process can be used to realize quantum state transfer [60]. Moreover, we give the general equations that should be satisfied by the optimal pump and Stokes fields. This means that optimal STIRAP can be con-

*xiaoliantuan@tyut.edu.cn

veniently combined with the quantum optimal control theory (QOCT) [61,62], which provides a systematic method for driving quantum systems in the best way possible. STIRAP protocols based on QOCT have been proposed in recent years [7,44]. Combining optimal STIRAP based on the geometric method with QOCT may improve the robustness of STIRAP while reducing the computational overhead of the optimization algorithm.

In optimal STIRAP, we use a dynamical quantum geometric tensor [59] that takes a similar form to the quantum geometric tensor [63]. The dynamical quantum geometric tensor can quantify the overall nonadiabatic transition rate and guide the optimization process. By keeping the overall nonadiabatic transition rate constant during the evolution process, the nonadiabatic effects are periodically self-eliminated in the adiabatic passage, and the adiabatic evolution can be achieved in appreciably short times. In order to realize accelerated adiabatic population transfer, we give the optimal control protocol of STIRAP in the case of large intermediate-level detuning and single-photon resonance. Specifically, in the case of large detuning, we first map STIRAP to a Landau-Zener-type transition in the effective two-level system by using adiabatic elimination, then optimize the Landau-Zener-type transition by the geometric method, and finally obtain the optimal pump and Stokes pulses for fast STIRAP. In the case of single-photon resonance, the optimal pulses are obtained by solving the optimization equation directly. Optimal STIRAP does not require additional couplings, and accelerated adiabatic population transfer can be implemented by modifying the pump and Stokes pulses. Furthermore, as an accelerated adiabatic passage, optimal STIRAP is not only robust against small variations of experimental parameters but also avoids decoherence resulting from long-time evolution. We numerically simulate the performance of optimal STIRAP and compare it with conventional STIRAP and stimulated Raman transition (SRT). The results show that optimal STIRAP can achieve fast and robust population transfer within shorter operation times.

II. GEOMETRIC OPTIMIZATION OF ADIABATIC PASSAGE

In this section, we shall briefly introduce the geometric method to optimize the finite-time adiabatic passage of quantum systems [59]. Consider an N -dimensional quantum system defined by the time-dependent Hamiltonian $H(t)$, with its instantaneous eigenvalues $\{E_n(t)\}$ and nondegenerate eigenstates $\{|E_n(t)\rangle\}$. According to the adiabatic theorem [21–23], if $H(t)$ varies slowly enough, the system initially in the n -th eigenstate $|E_n(0)\rangle$ will evolve along the instantaneous eigenstate $|E_n(t)\rangle$ up to a phase factor. However, the adiabatic evolution strictly holds only for an infinitely slow process that needs infinite running time. For finite-time evolution processes, the nonadiabatic transitions will make the time-evolving state deviate from the adiabatic eigenstate.

To evaluate the amount of nonadiabatic transitions, the time-evolving state can be expanded in the adiabatic frame $|\psi_n(t)\rangle = \sum_l c_{nl}(t)|E_l(t)\rangle$. The Schrödinger equation $i\partial_t|\psi(t)\rangle = H(t)|\psi(t)\rangle$ reduces to equations for the state

amplitudes $c_{nl}(t)$

$$\frac{\partial c_{nl}}{\partial t} = -ic_{nl}E_l(t) - \sum_m c_{nm}\langle E_l(t)|\frac{\partial}{\partial t}|E_m(t)\rangle. \quad (2)$$

The amount of nonadiabatic transitions from the adiabatic eigenstate $|E_n(t)\rangle$ can be quantified as the nonadiabatic transition probability $P_n^T(t) = \sum_{l \neq n} |c_{nl}(t)|^2$. According to the high-order adiabatic approximation theory [64–67], the first-order term of $P_n^T(t)$ is bounded by $P_{n,-}^T(t) \leq P_n^T(t) \leq P_{n,+}^T(t)$, with

$$P_{n,\pm}^T(t) = \frac{1}{\tau^2} \sum_{l \neq n} \left[\left| \tilde{T}_{nl}\left(\frac{t}{\tau}\right) \right| \pm |\tilde{T}_{nl}(0)| \right]^2, \quad (3)$$

in which τ is the total time of the evolution process, and \tilde{T}_{nl} are the nonadiabatic transition rates and take the form of

$$\tilde{T}_{nl}(s) = \frac{\langle \tilde{E}_l(s) | \frac{\partial}{\partial s} | \tilde{E}_n(s) \rangle}{\tilde{E}_n(s) - \tilde{E}_l(s)}, \quad (4)$$

with the rescaled time $s = t/\tau$, and the tildes are used to denote the functions of s . The overall nonadiabatic transition rate is defined as $\tilde{T}_n(s) := [\sum_{l \neq n} |\tilde{T}_{nl}(s)|^2]^{1/2}$. Considering that the case of the Hamiltonian $H = H[\vec{\lambda}(s)]$ is time dependent through multiple parameters $\vec{\lambda}(s) = \{\lambda_i(s)\}$, the overall nonadiabatic transition rate can be calculated by the dynamical quantum geometric tensor

$$\tilde{T}_n(s) = \left[\sum_{i,j} (\text{Re} D_{n,ij}) \frac{\partial \lambda_i}{\partial s} \frac{\partial \lambda_j}{\partial s} \right]^{\frac{1}{2}}, \quad (5)$$

in which $D_{n,ij}$ is the dynamical quantum geometric tensor

$$D_{n,ij} = \sum_{l \neq n} \frac{\langle \tilde{E}_l | \frac{\partial H}{\partial \lambda_i} | \tilde{E}_n \rangle \langle \tilde{E}_n | \frac{\partial H}{\partial \lambda_j} | \tilde{E}_l \rangle}{(\tilde{E}_n - \tilde{E}_l)^4}. \quad (6)$$

The optimal protocol for finite-time adiabatic passage is to keep constant $\tilde{T}_n(s)$ during the evolution process,

$$\tilde{T}_n(s) = \text{const.}, \quad (7)$$

which makes the time-evolving state deviate from the adiabatic eigenstate uniformly and back to the adiabatic eigenstate at the resonance points. The upper bound of nonadiabatic transition probability in Eq. (3) becomes $P_{n,+}^T = 4\tilde{T}_n^2(s)/\tau^2$. Therefore, the adiabatic control protocol designed according to Eq. (7) can reach quantum adiabaticity in appreciably shorter times.

III. OPTIMIZATION OF STIRAP

Considering a three-level system with states $|1\rangle$, $|2\rangle$, and $|3\rangle$, our goal is to realize fast population transfer from the starting state $|1\rangle$ to the final state $|3\rangle$ by optimized STIRAP. In this section, we shall propose the optimal protocol for STIRAP.

As a paradigmatic model, the Hamiltonian for STIRAP under rotating wave approximation takes the form of

$$H(t) = \frac{\hbar}{2} \begin{pmatrix} 0 & \Omega_p(t) & 0 \\ \Omega_p(t) & 2\Delta & \Omega_s(t) \\ 0 & \Omega_s(t) & 2\delta \end{pmatrix}, \quad (8)$$

where $\Omega_p(t)$ and $\Omega_s(t)$ are the Rabi frequencies of pump and Stokes fields. The detunings from resonance are defined as $\Delta_p = (E_2 - E_1)/\hbar - \omega_p$, $\Delta_s = (|E_2 - E_3|)/\hbar - \omega_s$, with E_j , where $j = 1, 2, 3$, are the bare-basis-state energies. The single-photon detuning is $\Delta = \Delta_p$. The two-photon detuning is $\delta = \Delta_p - \Delta_s$ for the Λ configuration and $\delta = \Delta_p + \Delta_s$ for the ladder configuration.

On two-photon resonance ($\delta = 0$), the Hamiltonian in Eq. (8) has a zero-eigenvalue eigenstate, called dark state

$$|E_0(t)\rangle = \cos\theta(t)|1\rangle - \sin\theta(t)|3\rangle, \quad (9)$$

where the mixing angle $\theta(t)$ is defined as

$$\theta(t) = \arctan \frac{\Omega_p(t)}{\Omega_s(t)}. \quad (10)$$

In STIRAP protocol, the Rabi frequencies of pump and Stokes fields is set to satisfy the following conditions:

$$\lim_{t \rightarrow 0} \frac{\Omega_p(t)}{\Omega_s(t)} = 0, \quad \lim_{t \rightarrow \tau} \frac{\Omega_s(t)}{\Omega_p(t)} = 0. \quad (11)$$

Obviously, under these conditions, the mixing angle $\theta(t)$ approaches 0 and $\pi/2$ at the initial time and final time, respectively. The dark state $|E_0(t)\rangle$ adiabatically connects the initial state $|1\rangle$ and target state $|3\rangle$. Therefore, population transfer from $|1\rangle$ to $|3\rangle$ can be realized by the adiabatic evolution along the dark state $|E_0(t)\rangle$.

The local condition for adiabatic evolution during STIRAP reads $\Omega_{\text{rms}} \gg |\dot{\theta}(t)|$, with $\Omega_{\text{rms}} = [\Omega_p^2(t) + \Omega_s^2(t)]^{1/2}$. By integrating the local condition, the global condition is given as $A = \int_0^\tau \Omega_{\text{rms}}(t) dt \gg \pi/2$. A is the rms pulse area, which is proportional to the peak Rabi frequency Ω_{max} and the pulse duration τ , i.e., $A \propto \Omega_{\text{max}} \tau$. The global adiabatic condition demands that the pulse intensities and the pulse durations must be large enough [5]. As a rough estimate neglecting the peculiarities of the nonadiabatic transition, achieving transfer fidelity more than 99.9% requires the rms pulse area $A > 30$ [56]. In real physical systems, such as atoms and molecules, there is always an upper limit to the peak Rabi frequency Ω_{max} . Therefore, the operation time of STIRAP must be sufficiently long in order to satisfy the adiabatic condition.

The conventional idealized description of STIRAP does not include the time dependence of the pump and Stokes fields, so it does not take the nonadiabatic effects associated with the temporal variation of the pump and Stokes fields into account [68]. In the following, we shall propose an optimized version of STIRAP based on the dynamical quantum geometric tensor, which adequately exploits the temporal variation of pump and Stokes fields. By using the optimal pump and Stokes fields, STIRAP can be realized in shorter operation times. We present the optimal protocol for STIRAP under different situations, including large detuning ($\Delta \gg \Omega$) and single-photon resonance ($\Delta = 0$).

A. At large detuning

At large intermediate-level detuning ($\Delta \gg \Omega$), the intermediate state $|2\rangle$ is scarcely populated. It can be eliminated adiabatically. As a result, the effective two-level Hamiltonian

in the subspace of levels $|1\rangle$ and $|3\rangle$ takes the form of

$$H_{\text{eff}} = \frac{\hbar}{2} \begin{pmatrix} -\Delta_{\text{eff}}(t) & \Omega_{\text{eff}}(t) \\ \Omega_{\text{eff}}(t) & \Delta_{\text{eff}}(t) \end{pmatrix}, \quad (12)$$

where the effective Rabi frequency $\Omega_{\text{eff}}(t)$ and detuning $\Delta_{\text{eff}}(t)$ are given by

$$\begin{aligned} \Omega_{\text{eff}}(t) &= -\frac{\Omega_p(t)\Omega_s(t)}{2\Delta}, \\ \Delta_{\text{eff}}(t) &= \frac{\Omega_p^2(t) - \Omega_s^2(t)}{4\Delta}. \end{aligned} \quad (13)$$

In this case, STIRAP can be regarded as a Landau-Zener-type transition in the effective two-level system [69]. Thus, we consider the Landau-Zener model described by the Hamiltonian

$$H_{\text{LZ}}(t) = \frac{\hbar\Omega(t)}{2} \begin{pmatrix} \lambda(t) & 1 \\ 1 & -\lambda(t) \end{pmatrix}, \quad (14)$$

where $\Omega(t)$ and $\lambda(t)$ are the time-dependent control parameters. The instantaneous eigenstates of $H_{\text{LZ}}(t)$ are

$$\begin{aligned} |E_g(t)\rangle &= -\sqrt{\frac{\sqrt{1+\lambda^2}-\lambda}{2\sqrt{1+\lambda^2}}} |1\rangle + \sqrt{\frac{\sqrt{1+\lambda^2}+\lambda}{2\sqrt{1+\lambda^2}}} |3\rangle, \\ |E_e(t)\rangle &= \sqrt{\frac{\sqrt{1+\lambda^2}+\lambda}{2\sqrt{1+\lambda^2}}} |1\rangle + \sqrt{\frac{\sqrt{1+\lambda^2}-\lambda}{2\sqrt{1+\lambda^2}}} |3\rangle, \end{aligned} \quad (15)$$

corresponding to eigenvalues $E_g(t) = -\hbar\Omega\sqrt{1+\lambda^2}/2$ and $E_e(t) = \hbar\Omega\sqrt{1+\lambda^2}/2$, respectively. Substituting the Hamiltonian (14), instantaneous eigenvalues, and eigenstates into Eq. (6), we obtain the components of the dynamical quantum geometric tensor

$$\begin{aligned} D_{g,\lambda\lambda} &= \frac{1}{4\hbar^2\Omega^2(1+\lambda^2)^3}, \\ D_{g,\Omega\Omega} &= D_{g,\Omega\lambda} = D_{g,\lambda\Omega} = 0. \end{aligned} \quad (16)$$

According to Eqs. (5) and (7), the equation that the optimal protocol needs to satisfy reads

$$\frac{\dot{\tilde{\lambda}}(s)}{2\hbar\tilde{\Omega}(s)[1+\tilde{\lambda}^2(s)]^{\frac{3}{2}}} = \text{const.}, \quad (17)$$

where the rescaled time $s \in [0, 1]$, and the dot above the symbol represents the derivative with respect to s . The solutions of the above equation are not unique, and here we present one of them. For the initial and final values of the control parameter $\tilde{\lambda}(0) = -4$ and $\tilde{\lambda}(1) = 4$, $\tilde{\lambda}(s)$ and $\tilde{\Omega}(s)$ can be set as

$$\begin{aligned} \tilde{\lambda}(s) &= 8s - 4, \\ \tilde{\Omega}(s) &= 0.4[1 + (8s - 4)^2]^{-\frac{3}{2}}, \end{aligned} \quad (18)$$

which satisfies Eq. (17). The constant in Eq. (17) is the overall nonadiabatic transition rate, which represents the extent of the time-evolving state deviating from the adiabatic eigenstate. In theory, the smaller the constant is, the less time it takes to achieve quantum adiabaticity. However, a larger peak Rabi frequency is required to make the overall nonadiabatic transition rate smaller. Thus, we should choose appropriate constants to obtain experimentally achievable pulses. For the solution in Eq. (18), the constant is set as $10/\hbar$.

Until now, we have obtained the optimal control protocol for the effective two-level system. Therefore, we can go back to the three-level system and obtain the optimal pump and Stokes fields by comparing the Hamiltonian in Eqs. (12) and (14). Solving the two equations for Ω_p and Ω_s in Eq. (13), we can express them in terms of Ω_{eff} and Δ_{eff} ,

$$\begin{aligned}\Omega_p &= [2\Delta(\sqrt{\Omega_{\text{eff}}^2 + \Delta_{\text{eff}}^2} + \Delta_{\text{eff}})]^{1/2}, \\ \Omega_s &= [2\Delta(\sqrt{\Omega_{\text{eff}}^2 + \Delta_{\text{eff}}^2} - \Delta_{\text{eff}})]^{1/2}.\end{aligned}\quad (19)$$

Substituting $\tilde{\Omega}_{\text{eff}}(s) = \tilde{\Omega}(s)$ and $\tilde{\Delta}_{\text{eff}}(s) = -\tilde{\Omega}(s)\tilde{\lambda}(s)$ into the above equation, we obtain the optimal pump pulse $\tilde{\Omega}_p(s)$ and Stokes pulse $\tilde{\Omega}_s(s)$ for implementing optimal STIRAP at large intermediate-level detuning.

To illustrate the superiority of the optimal control protocol, we simulate the performance of optimal STIRAP and compare it with conventional STIRAP using Gaussian pulses. We set the operation time $\tau = 35 \mu\text{s}$ and the intermediate-level detuning $\Delta = 1 \text{ GHz}$. According to Eqs. (18) and (19), we can obtain the Rabi frequencies of pump field $\Omega_p(t)$ and Stokes field $\Omega_s(t)$ for optimal STIRAP, as shown in Fig. 1(a). The maximum amplitude of $\Omega_p(t)$ and $\Omega_s(t)$ is $\Omega_0 = 30.79 \text{ MHz}$. By using these optimal pulses, the perfect population transfer from $|1\rangle$ to $|3\rangle$ can be achieved within the operation time, as shown in Fig. 1(b). Then, we simulate the performance of STIRAP using Gaussian pulses. We set the Rabi frequencies of the pump and Stokes fields as

$$\begin{aligned}\Omega_p(t) &= \Omega_0 \exp\left[-\frac{(t - \tau/2 - \mu)^2}{\sigma^2}\right], \\ \Omega_s(t) &= \Omega_0 \exp\left[-\frac{(t - \tau/2 + \mu)^2}{\sigma^2}\right],\end{aligned}\quad (20)$$

where the operation time $\tau = 35 \mu\text{s}$ and the maximum amplitude of Rabi frequencies $\Omega_0 = 30.79 \text{ MHz}$ are the same as in the optimal protocol, full width at half maximum $\sigma = \tau/6$, and separation time between the two pulses $\mu = \tau/10$, as shown in Fig. 1(c). The perform of STIRAP using Gaussian pulses with $\tau = 35 \mu\text{s}$ is shown in Fig. 1(d). Under the conditions of the same operation time and the same maximum amplitude of Rabi frequencies, the evolution driven by Gaussian pulses is not adiabatic at all, so the population transfer from $|1\rangle$ to $|3\rangle$ is incomplete. The relation between the infidelity $1 - P_3(\tau)$ and the operation time τ is shown in Fig. 2, where $P_3(\tau)$ is the population of state $|3\rangle$ at final time. As shown in Fig. 2, there are some time windows represented by the blue shaded regions on the horizontal axis; by choosing the pulse duration τ in the time windows, the infidelity of optimal STIRAP can be kept below 10^{-3} . In the first time window, the infidelity of optimal STIRAP drops below 10^{-3} at $\tau = 35 \mu\text{s}$, while conventional STIRAP using Gaussian pulses needs operation time more than $180 \mu\text{s}$ to reach the same level of infidelity. So, the simulation results show the superiority of the optimal control protocol for realizing population transfer in shorter operation times.

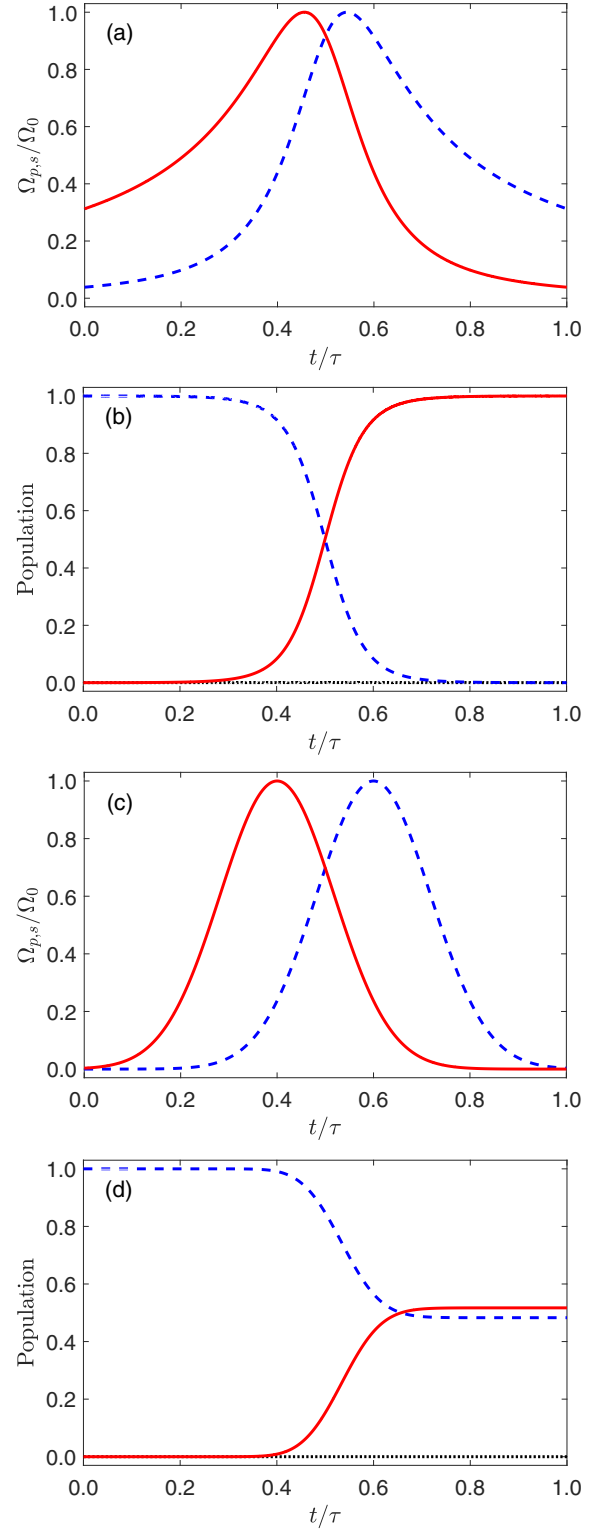


FIG. 1. The shape of pulses and performance of the population transfers. (a) Rabi frequencies of the Stokes field (solid red) and pump field (dashed blue) for optimal STIRAP. (b) Performance of optimal STIRAP, where the populations of levels $|1\rangle$ (dashed blue), $|2\rangle$ (dotted black), and $|3\rangle$ (solid red) are presented. (c) Rabi frequencies of the Stokes field and pump field for STIRAP using Gaussian pulses. (d) Performance of STIRAP using Gaussian pulses. Parameters: $\Omega_0 = 30.79 \text{ MHz}$, $\Delta = 1 \text{ GHz}$, $\tau = 35 \mu\text{s}$, $\sigma = \tau/6$, and $\mu = \tau/10$.

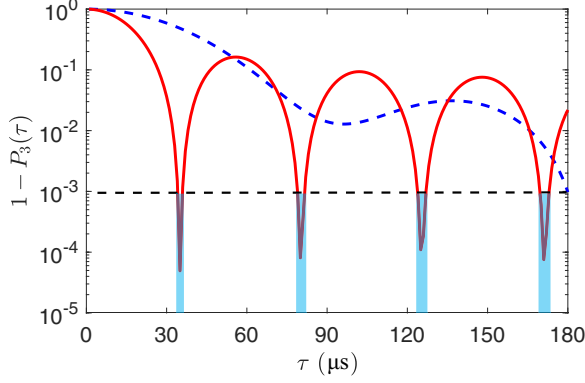


FIG. 2. Infidelity $1 - P_3(\tau)$ plotted as a function of the operation time τ at large intermediate-level detuning for optimal STIRAP (solid red) and STIRAP using Gaussian pulses (dashed blue). Time windows to get $1 - P_3(\tau) < 10^{-3}$ are indicated by the blue shaded regions for optimal STIRAP.

B. Single-photon resonance

On single-photon resonance ($\Delta = 0$), the STIRAP Hamiltonian reads as

$$H(t) = \frac{\hbar}{2} \begin{pmatrix} 0 & \Omega_p(t) & 0 \\ \Omega_p(t) & 0 & \Omega_s(t) \\ 0 & \Omega_s(t) & 0 \end{pmatrix}, \quad (21)$$

whose instantaneous eigenstates are

$$\begin{aligned} |E_+(t)\rangle &= \frac{1}{\sqrt{2}}(\sin\theta(t)|1\rangle + |2\rangle + \cos\theta(t)|3\rangle), \\ |E_0(t)\rangle &= \cos\theta(t)|1\rangle - \sin\theta(t)|3\rangle, \\ |E_-(t)\rangle &= \frac{1}{\sqrt{2}}(\sin\theta(t)|1\rangle - |2\rangle + \cos\theta(t)|3\rangle), \end{aligned} \quad (22)$$

with eigenvalues $E_+(t) = \hbar\Omega_{\text{rms}}/2$, $E_0(t) = 0$, $E_-(t) = -\hbar\Omega_{\text{rms}}/2$. The mixing angle $\theta(t) = \arctan[\Omega_p(t)/\Omega_s(t)]$ and $\Omega_{\text{rms}} = [\Omega_p^2(t) + \Omega_s^2(t)]^{1/2}$. By using Eq. (6) we can obtain the components of the dynamical quantum geometric tensor

$$\begin{aligned} D_{0,pp} &= \frac{4\Omega_s^2}{\hbar^2(\Omega_p^2 + \Omega_s^2)^3}, & D_{0,ps} &= \frac{-4\Omega_p\Omega_s}{\hbar^2(\Omega_p^2 + \Omega_s^2)^3}, \\ D_{0,sp} &= \frac{-4\Omega_p\Omega_s}{\hbar^2(\Omega_p^2 + \Omega_s^2)^3}, & D_{0,ss} &= \frac{4\Omega_p^2}{\hbar^2(\Omega_p^2 + \Omega_s^2)^3}. \end{aligned} \quad (23)$$

According to Eq. (7), the optimal pump pulse $\tilde{\Omega}_p(s)$ and Stokes pulse $\tilde{\Omega}_s(s)$ satisfy the equation

$$\frac{4(\tilde{\Omega}_p^2\dot{\tilde{\Omega}}_s^2 - 2\tilde{\Omega}_p\dot{\tilde{\Omega}}_s\dot{\tilde{\Omega}}_s\dot{\tilde{\Omega}}_p + \dot{\tilde{\Omega}}_p^2\tilde{\Omega}_s^2)^{\frac{1}{2}}}{\hbar(\tilde{\Omega}_p^2 + \tilde{\Omega}_s^2)^{\frac{3}{2}}} = \text{const.} \quad (24)$$

Moreover, to ensure the realization of population transfer, $\tilde{\Omega}_p(s)$ and $\tilde{\Omega}_s(s)$ must satisfy the conditions in Eq. (11). In this case, the simplest solution of Eq. (24) is

$$\tilde{\Omega}_p(s) = \Omega_0 \sin\left(\frac{\pi}{2}s\right), \quad \tilde{\Omega}_s(s) = \Omega_0 \cos\left(\frac{\pi}{2}s\right), \quad (25)$$

where Ω_0 is the maximum amplitude of Rabi frequencies. Substituting Eq. (25) into Eqs. (7) and (24), we obtain the

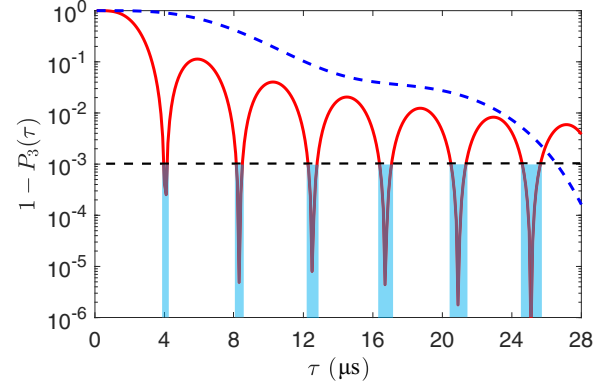


FIG. 3. Infidelity $1 - P_3(\tau)$ plotted as a function of the operation time τ on single-photon resonance for optimal STIRAP (solid red) and STIRAP using Gaussian pulses (dashed blue). Time windows to get $1 - P_3(\tau) < 10^{-3}$ are indicated by blue shaded regions for the optimal STIRAP.

trade-off between the Rabi frequencies, and the overall nonadiabatic transition rate reads $\tilde{T}_n(s) = 4/\hbar\Omega_0$. In order to make the overall adiabatic transition as small as possible, the Rabi frequencies can be set as the maximum that can be achieved.

We compare the performance of the optimal STIRAP with STIRAP using Gaussian pulses by numerical simulation. The maximum amplitude of $\Omega_p(t)$ and $\Omega_s(t)$ is set as $\Omega_0 = 3\text{MHz}$. The Gaussian pulses take the form of Eq. (20), the maximum amplitude of Rabi frequencies $\Omega_0 = 3\text{MHz}$, full width at half maximum $\sigma = \tau/6$, and separation time between the two pulses $\mu = \tau/10$. The relation between the infidelity $1 - P_3(\tau)$ and the operation time τ is shown in Fig. 3. By choosing the pulse duration τ in the time windows on the horizontal axis, the infidelity of optimal STIRAP can be kept below 10^{-3} . The infidelity of optimal STIRAP drops below 10^{-3} at $\tau = 4\ \mu\text{s}$ for the first time, while conventional STIRAP using Gaussian pulses needs operation time of more than $26\ \mu\text{s}$ to reach the same level. Moreover, the optimal STIRAP is always superior to conventional STIRAP using Gaussian pulses in short operation times.

IV. DISCUSSION

In this section, we first discuss the relation between the infidelity $1 - P_3(\tau)$ and the operation time τ for the optimal STIRAP developed in this paper and for STIRAP using Gaussian pulses, as shown in Figs. 2 and 3. These results show the superiority of the optimal protocol. Furthermore, it is worth noting that there are some points of resonance where the infidelity plummets to zero, which is because the nonadiabatic transitions are regularized by keeping a constant overall nonadiabatic transition rate during the evolution, and the evolving state in the adiabatic frame undergoes periodic evolution and back to the adiabatic eigenstate at the resonance points. In other words, the nonadiabatic effects are self-eliminating in the optimal adiabatic passage. This adiabatic resonance phenomenon is first discovered in the adiabatic quantum teleportation protocol [70]. Essentially, keeping a constant overall nonadiabatic transition rate [Eq. (7)] is the general condition for achieving adiabatic resonance. As shown in Fig. 3, there

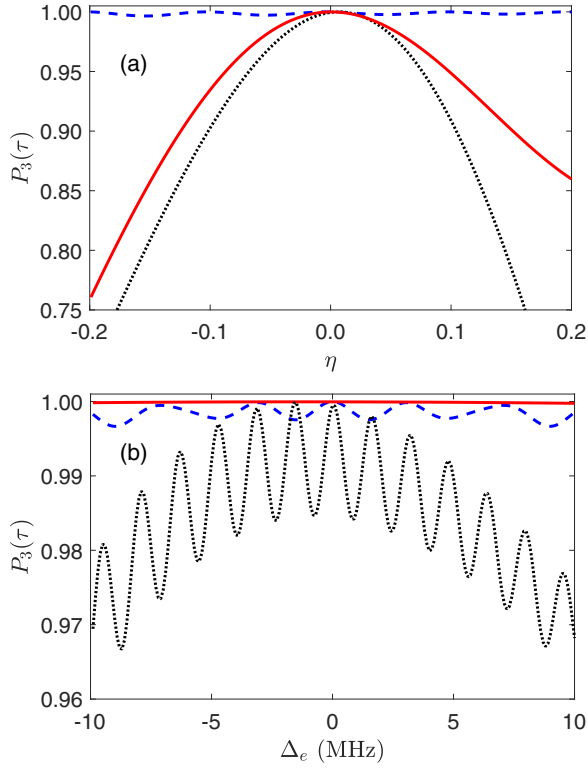


FIG. 4. (a) Population of state $|3\rangle$ at final time plotted as a function of the systematic Rabi frequency error for optimal STIRAP at large detuning with $\tau = 35 \mu\text{s}$ (solid red), optimal STIRAP on single-photon resonance with $\Omega_0 = 30 \text{ MHz}$ and $\tau = 4.2 \mu\text{s}$ (dashed blue), and SRT with $\Delta_{\text{srt}} = 100 \text{ MHz}$, $\Omega_{\text{srt1}} = \Omega_{\text{srt3}} = \sqrt{50\pi} \text{ MHz}$ and $\tau = 4 \mu\text{s}$ (dotted black). (b) Population of state $|3\rangle$ at final time plotted as a function of the detuning error for optimal STIRAP at large detuning (solid red), optimal STIRAP on single-photon resonance (dashed blue), and SRT (dotted black).

are some time windows near the resonance point. Within these time windows, one can implement fast and accurate population transfer. The length of the time windows increases with the operation time. It means that optimal STIRAP is robust against small variations of pulse timing.

Then, we turn to discuss the robustness of optimal STIRAP against different systematic errors. To this end, we numerically simulate the perform of optimal STIRAP under the influence of systematic error and compare it with SRT [71], a popularly used technology for fast population transfer. SRT is realized by applying two highly detuned driving fields with the intermediate-level detuning Δ_{srt} and Rabi frequency $\Omega_{\text{srt1}} = \Omega_{\text{srt3}}$. At large intermediate-level detuning, according to Eq. (12), the system reduces to a two-level system consisting of levels $|1\rangle$ and $|3\rangle$ with an effective Rabi frequency $\Omega_{\text{srt}} = -\Omega_{\text{srt1}}\Omega_{\text{srt3}}/2\Delta_{\text{srt}}$. Then, the fast population transfer between states $|1\rangle$ and $|3\rangle$ can be implemented. Here, we set $\Delta_{\text{srt}} = 100 \text{ MHz}$ and $\Omega_{\text{srt1}} = \Omega_{\text{srt3}} = \sqrt{50\pi} \text{ MHz}$, and the population transfer from $|1\rangle$ and $|3\rangle$ can be approximately implemented at $\tau = 4 \mu\text{s}$. The simulation results are shown in Fig. 4. Figure 4(a) shows the robustness against the systematic Rabi frequency error when the Rabi frequencies of the pump and Stokes fields change from Ω_p and Ω_s to $\Omega_p(1 + \eta)$ and

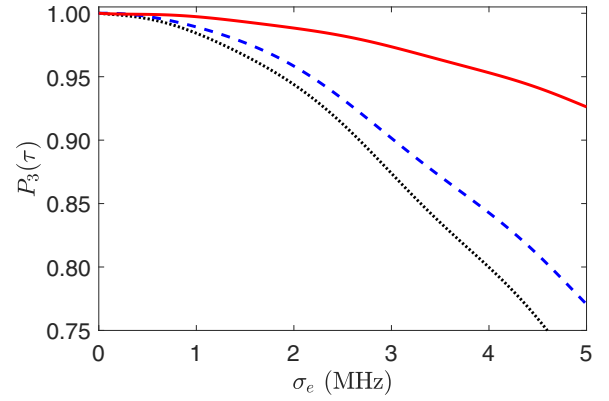


FIG. 5. Population of state $|3\rangle$ at final time plotted as a function of the strength of random Rabi frequency errors for optimal STIRAP at large detuning (solid red), optimal STIRAP on single-photon resonance (dashed blue), and SRT (dotted black). The parameters are the same as in Fig. 4.

$\Omega_s(1 + \eta)$. As one sees, optimal STIRAP has better robustness against the systematic Rabi frequency error than SRT. Particularly, on single-photon resonance, the final population of optimal STIRAP is almost unaffected by the vibration of Rabi frequencies. Figure 4(b) shows the robustness against the detuning error, when the single-photon detuning changes from Δ to $\Delta + \Delta_e$. It can be seen that the robustness of optimal STIRAP against the detuning error is much better than that of SRT. At large intermediate-level detuning, the results of optimal STIRAP are not affected by small vibration of detuning.

Finally, we consider the robustness of optimal STIRAP against random errors that make the time shapes of the pump and Stokes pulses deviate from the ideal pulses. We model the time-dependent perturbation of Rabi frequencies by Ornstein-Uhlenbeck processes [72], where perturbation $\varepsilon_e(t)$ is a random variable obtained by solving the Ornstein-Uhlenbeck equation

$$d\varepsilon_e = -\frac{\varepsilon_e - \mu_e}{\tau_e} dt + \sigma_e \sqrt{\frac{2}{\tau_e}} dW, \quad (26)$$

in which μ_e is the mean, σ_e is the standard deviation, τ_e is the correlation time, and W is the standard Wiener process. Here, we set $\tau_e = 1 \mu\text{s}$ and $\mu_e = 0$; the value of the standard deviation σ_e indicates the strength of random errors. We numerically simulate the performance of optimal STIRAP when the Rabi frequencies of the pump and Stokes fields change from Ω_p and Ω_s to $\Omega_p + \varepsilon_e$ and $\Omega_s + \varepsilon_e$, and compare it with SRT. As shown in Fig. 5, the robustness of optimal STIRAP against the random Rabi frequency error is better than SRT. Therefore, optimal STIRAP is robust against the random variation of the time shapes of the pump and Stokes pulses.

V. CONCLUSION

In conclusion, we have shown how to realize accelerated adiabatic population transfer between two quantum states by using the geometric method to optimize finite-time adiabatic passage. In optimal STIRAP, the nonadiabatic effects

resulting from fast evolution are eliminated by keeping the overall nonadiabatic transition rate constant during the evolution process. Thus, accurate population transfer can be implemented at appreciably shorter times. We concentrate on two cases of large detuning and single-photon resonance and give the optimal shapes of pump and Stokes pulses to implement fast population transfer. We numerically simulate the performance of optimal STIRAP and compare it with conventional STIRAP using Gaussian pulses. The results show that the evolution time of optimal STIRAP is about six times shorter than that of conventional STIRAP under the premise of achieving the same fidelity. Moreover, we numerically simulate the perform of optimal STIRAP under the influence of different types of errors and compare it with SRT. The numerical results clearly show that the robustness of optimal STIRAP against the systematic and random errors is better

than SRT. Therefore, optimal STIRAP not only avoids decoherence resulting from long time evolution but is also robust against small variations of experimental parameters. Optimal STIRAP is a promising protocol to achieve high-fidelity population transfer. We hope optimal STIRAP can shed light on accurate population transfer in quantum computation and quantum sensing.

ACKNOWLEDGMENTS

K.Z.L. and L.T.X. gratefully acknowledge support from the National Natural Science Foundation of China (Grants No. 62127817 and No. U23A20380). J.Z.T. gratefully acknowledge supports from the Science Foundation for Youths of Shanxi Province (Grant No. 202203021222113) and National Natural Science Foundation of China (Grant No. 62305241).

-
- [1] U. Gaubatz, P. Rudecki, S. Schiemann, and K. Bergmann, Population transfer between molecular vibrational levels by stimulated Raman scattering with partially overlapping laser fields. A new concept and experimental results, *J. Chem. Phys.* **92**, 5363 (1990).
- [2] K. Bergmann, H. Theuer, and B. W. Shore, Coherent population transfer among quantum states of atoms and molecules, *Rev. Mod. Phys.* **70**, 1003 (1998).
- [3] P. Král, I. Thanopoulos, and M. Shapiro, *Colloquium*: Coherently controlled adiabatic passage, *Rev. Mod. Phys.* **79**, 53 (2007).
- [4] K. Bergmann, N. V. Vitanov, and B. W. Shore, Perspective: Stimulated Raman adiabatic passage: The status after 25 years, *J. Chem. Phys.* **142**, 170901 (2015).
- [5] N. V. Vitanov, A. A. Rangelov, B. W. Shore, and K. Bergmann, Stimulated Raman adiabatic passage in physics, chemistry, and beyond, *Rev. Mod. Phys.* **89**, 015006 (2017).
- [6] D. A. Golter and H. L. Wang, Optically driven Rabi oscillations and adiabatic passage of single electron spins in diamond, *Phys. Rev. Lett.* **112**, 116403 (2014).
- [7] J. Z. Tian, T. Y. Du, Y. Liu, H. B. Liu, F. Z. Jin, R. S. Said, and J. M. Cai, Optimal quantum optical control of spin in diamond, *Phys. Rev. A* **100**, 012110 (2019).
- [8] F. Böhm, N. Nikolay, S. Neinert, C. E. Nebel, and O. Benson, Ground-state microwave-stimulated Raman transitions and adiabatic spin transfer in the ^{15}N nitrogen vacancy center, *Phys. Rev. B* **104**, 035201 (2021).
- [9] M. Gong, M. Yu, R. Betzholtz, Y. Chu, P. Yang, Z. Wang, and J. Cai, Accelerated quantum control in a three-level system by jumping along the geodesics, *Phys. Rev. A* **107**, L040602 (2023).
- [10] J. Chathanathil, A. Ramaswamy, V. S. Malinovsky, D. Budker, and S. A. Malinovskaya, Chirped fractional stimulated Raman adiabatic passage, *Phys. Rev. A* **108**, 043710 (2023).
- [11] K. S. Kumar, A. Vepsäläinen, S. Danilin, and G. S. Paraoanu, Stimulated Raman adiabatic passage in a three-level superconducting circuit, *Nat. Commun.* **7**, 10628 (2016).
- [12] H. K. Xu, C. Song, W. Y. Liu, G. M. Xue, F. F. Su, H. Deng, Y. Tian, D. N. Zheng, S. Han, Y. P. Zhong, H. Wang, Y.-X. Liu, and S. P. Zhao, Coherent population transfer between uncoupled or weakly coupled states in ladder-type superconducting qutrits, *Nat. Commun.* **7**, 11018 (2016).
- [13] W. Zheng, Y. Zhang, Y. Dong, J. Xu, Z. Wang, X. Wang, Y. Li, D. Lan, J. Zhao, S. Li, X. Tan, and Y. Yu, Optimal control of stimulated Raman adiabatic passage in a superconducting qutrit, *npj Quantum Inform.* **8**, 9 (2022).
- [14] X. Xu, B. Sun, P. R. Berman, D. G. Steel, A. S. Bracker, D. Gammon, and L. J. Sham, Coherent population trapping of an electron spin in a single negatively charged quantum dot, *Nat. Phys.* **4**, 692 (2008).
- [15] J. Houel, J. H. Prechtel, A. V. Kuhlmann, D. Brunner, C. E. Kuklewicz, B. D. Gerardot, N. G. Stoltz, P. M. Petroff, and R. J. Warburton, High resolution coherent population trapping on a single hole spin in a semiconductor quantum dot, *Phys. Rev. Lett.* **112**, 107401 (2014).
- [16] N. Domenikou, I. Thanopoulos, D. Stefanatos, V. Yannopoulos, and E. Paspalakis, Stimulated Raman adiabatic passage in a quantum system near a plasmonic nanoparticle, *J. Phys. B: At. Mol. Opt. Phys.* **55**, 154002 (2022).
- [17] Y.-D. Wang and A. A. Clerk, Using interference for high fidelity quantum state transfer in optomechanics, *Phys. Rev. Lett.* **108**, 153603 (2012).
- [18] V. Fedoseev, F. Luna, I. Hedgepeth, W. Löffler, and D. Bouwmeester, Stimulated Raman adiabatic passage in optomechanics, *Phys. Rev. Lett.* **126**, 113601 (2021).
- [19] Y.-H. Liu, X.-L. Yin, J.-F. Huang, and J.-Q. Liao, Accelerated ground-state cooling of an optomechanical resonator via shortcuts to adiabaticity, *Phys. Rev. A* **105**, 023504 (2022).
- [20] F. Zou, J.-Q. Liao, and Y. Li, Dynamical emission of phonon pairs in optomechanical systems, *Phys. Rev. A* **105**, 053507 (2022).
- [21] M. Born and V. Fock, Beweis des Adiabatenatzes, *Z. Phys.* **51**, 165 (1928).
- [22] A. Messiah, *Quantum Mechanics* (North-Holland, Amsterdam, 1962).
- [23] D. M. Tong, Quantitative condition is necessary in guaranteeing the validity of the adiabatic approximation, *Phys. Rev. Lett.* **104**, 120401 (2010).
- [24] E. Torrontegui, S. Ibáñez, S. Martínez-Garaot, M. Modugno, A. del Campo, D. Guéry-Odelin, A. Ruschhaupt, X. Chen, and J. G. Muga, Chapter 2—Shortcuts to adiabaticity, *Adv. At. Mol. Opt. Phys.* **62**, 117 (2013).

- [25] D. Guéry-Odelin, A. Ruschhaupt, A. Kiely, E. Torrontegui, S. Martínez-Garaot, and J. G. Muga, Shortcuts to adiabaticity: Concepts, methods, and applications, *Rev. Mod. Phys.* **91**, 045001 (2019).
- [26] X. Chen, I. Lizuain, A. Ruschhaupt, D. Guéry-Odelin, and J. G. Muga, Shortcut to adiabatic passage in two- and three-level atoms, *Phys. Rev. Lett.* **105**, 123003 (2010).
- [27] D. Daems, A. Ruschhaupt, D. Sugny, and S. Guérin, Robust quantum control by a single-shot shaped pulse, *Phys. Rev. Lett.* **111**, 050404 (2013).
- [28] A. Baksic, H. Ribeiro, and A. A. Clerk, Speeding up adiabatic quantum state transfer by using dressed states, *Phys. Rev. Lett.* **116**, 230503 (2016).
- [29] X. Chen and J. G. Muga, Engineering of fast population transfer in three-level systems, *Phys. Rev. A* **86**, 033405 (2012).
- [30] A. Ruschhaupt, X. Chen, D. Alonso, and J. G. Muga, Optimally robust shortcuts to population inversion in two-level quantum systems, *New J. Phys.* **14**, 093040 (2012).
- [31] M. Lu, Y. Xia, L. T. Shen, J. Song, and N. B. An, Shortcuts to adiabatic passage for population transfer and maximum entanglement creation between two atoms in a cavity, *Phys. Rev. A* **89**, 012326 (2014).
- [32] Y. H. Chen, Y. Xia, Q. Q. Cheng, and J. Song, Fast and noise-resistant implementation of quantum phase gates and creation of quantum entangled states, *Phys. Rev. A* **91**, 012325 (2015).
- [33] Y. C. Li and X. Chen, Shortcut to adiabatic population transfer in quantum three-level systems: Effective two-level problems and feasible counterdiabatic driving, *Phys. Rev. A* **94**, 063411 (2016).
- [34] Y. X. Du, Z. T. Liang, Y. C. Li, X. X. Yue, Q. X. Lv, W. Huang, X. Chen, H. Yan, and S. L. Zhu, Experimental realization of stimulated Raman shortcut-to-adiabatic passage with cold atoms, *Nat. Commun.* **7**, 12479 (2016).
- [35] X. K. Song, Q. Ai, J. Qiu, and F. G. Deng, Physically feasible three-level transitionless quantum driving with multiple Schrödinger dynamics, *Phys. Rev. A* **93**, 052324 (2016).
- [36] B. B. Zhou, A. Baksic, H. Ribeiro, C. G. Yale, F. J. Heremans, P. C. Jerger, A. Auer, G. Burkard, A. A. Clerk, and D. D. Awschalom, Accelerated quantum control using superadiabatic dynamics in a solid-state lambda system, *Nat. Phys.* **13**, 330 (2017).
- [37] B. H. Huang, Y. H. Kang, Y. H. Chen, Q. C. Wu, J. Song, and Y. Xia, Fast quantum state engineering via universal SU(2) transformation, *Phys. Rev. A* **96**, 022314 (2017).
- [38] H. L. Mortensen, J. J. W. H. Sørensen, K. Mølmer, and J. F. Sherson, Fast state transfer in a Λ -system: A shortcut-to-adiabaticity approach to robust and resource optimized control, *New J. Phys.* **20**, 025009 (2018).
- [39] X. T. Yu, Q. Zhang, Y. Ban, and X. Chen, Fast and robust control of two interacting spins, *Phys. Rev. A* **97**, 062317 (2018).
- [40] D. Stefanatos and E. Paspalakis, Efficient generation of the triplet Bell state between coupled spins using transitionless quantum driving and optimal control, *Phys. Rev. A* **99**, 022327 (2019).
- [41] D. Stefanatos and E. Paspalakis, Resonant shortcuts for adiabatic rapid passage with only z-field control, *Phys. Rev. A* **100**, 012111 (2019).
- [42] K. Blekos, D. Stefanatos, and E. Paspalakis, Performance of superadiabatic stimulated Raman adiabatic passage in the presence of dissipation and Ornstein-Uhlenbeck dephasing, *Phys. Rev. A* **102**, 023715 (2020).
- [43] X. Shi and H. Q. Zhao, Effect of spontaneous emission on the shortcut to adiabaticity in three-state systems, *Phys. Rev. A* **104**, 052221 (2021).
- [44] V. Evangelakos, E. Paspalakis, and D. Stefanatos, Optimal STIRAP shortcuts using the spin-to-spring mapping, *Phys. Rev. A* **107**, 052606 (2023).
- [45] S. L. Wu, W. Ma, X. L. Huang, and X. X. Yi, Shortcuts to adiabaticity for open quantum systems and a mixed-state inverse engineering scheme, *Phys. Rev. Appl.* **16**, 044028 (2021).
- [46] X.-P. Dong, Z.-B. Feng, X.-J. Lu, M. Li, and Z.-Y. Zhao, Fast population transfer with a superconducting qutrit via non-Hermitian shortcut to adiabaticity, *Chin. Phys. B* **32**, 034201 (2023).
- [47] X. Laforgue, X. Chen, and S. Guérin, Robust stimulated Raman exact passage using shaped pulses, *Phys. Rev. A* **100**, 023415 (2019).
- [48] T. Xu, K. Liu, X. Chen, and S. Guérin, Invariant-based optimal composite stimulated Raman exact passage, *J. Phys. B* **52**, 235501 (2019).
- [49] X. K. Song, F. Meng, B. J. Liu, D. Wang, L. Ye, and M.-H. Yung, Robust stimulated Raman shortcut-to-adiabatic passage with invariant-based optimal control, *Opt. Express* **29**, 7998 (2021).
- [50] B. J. Liu and M. H. Yung, Coherent control with user-defined passage, *Quantum Sci. Technol.* **6**, 025002 (2021).
- [51] J. J. Niu, B. J. Liu, Y. X. Zhou, T. X. Yan, W. H. Huang, W. Y. Liu, L. B. Zhang, H. Jia, S. Liu, M. H. Yung, Y. Z. Chen, and D. P. Yu, Customizable quantum control via stimulated Raman user-defined passage, *Phys. Rev. Appl.* **17**, 034056 (2022).
- [52] X. Laforgue, G. Dridi, and S. Guérin, Optimal robust stimulated Raman exact passage by inverse optimization, *Phys. Rev. A* **105**, 032807 (2022).
- [53] K. Z. Li and G. F. Xu, Robust population transfer of spin states by geometric formalism, *Phys. Rev. A* **105**, 052433 (2022).
- [54] K. Liu, D. Sugny, X. Chen, and S. Guérin, Optimal pulse design for dissipative-stimulated Raman exact passage, *Entropy* **25**, 790 (2023).
- [55] H. Xu, X. K. Song, D. Wang, and L. Ye, Robust coherent control in three-level quantum systems using composite pulses, *Opt. Express* **30**, 3125 (2022).
- [56] G. S. Vasilev, A. Kuhn, and N. V. Vitanov, Optimum pulse shapes for stimulated Raman adiabatic passage, *Phys. Rev. A* **80**, 013417 (2009).
- [57] J. P. Davis and P. Pechukas, Nonadiabatic transitions induced by a time-dependent Hamiltonian in the semiclassical/adiabatic limit: The two-state case, *J. Chem. Phys.* **64**, 3129 (1976).
- [58] G. Dridi, S. Guérin, V. Hakobyan, H. R. Jauslin, and H. Eleuch, Ultrafast stimulated Raman parallel adiabatic passage by shaped pulses, *Phys. Rev. A* **80**, 043408 (2009).
- [59] J.-F. Chen, Speeding up quantum adiabatic processes with a dynamical quantum geometric tensor, *Phys. Rev. Res.* **4**, 023252 (2022).
- [60] R. R. Agundez, C. D. Hill, L. C. L. Hollenberg, S. Rogge, and M. Blaauboer, Superadiabatic quantum state transfer in spin chains, *Phys. Rev. A* **95**, 012317 (2017).
- [61] C. P. Koch, U. Boscain, T. Calarco, G. Dirr, S. Filipp, S. J. Glaser, R. Kosloff, S. Montangero, T. Schulte-Herbrüggen, D. Sugny, and F. K. Wilhelm, Quantum optimal control in quantum

- technologies. Strategic report on current status, visions and goals for research in Europe, *EPJ Quantum Technol.* **9**, 19 (2022).
- [62] S. J. Glaser, U. Boscain, T. Calarco, C. P. Koch, W. Köckenberger, R. Kosloff, I. Kuprov, B. Luy, S. Schirmer, T. Schulte-Herbrüggen, D. Sugny, and F. K. Wilhelm, Training Schrödinger's cat: Quantum optimal control, *Eur. Phys. J. D* **69**, 279 (2015).
- [63] J. P. Provost and G. Vallee, Riemannian structure on manifolds of quantum states, *Commun. Math. Phys.* **76**, 289 (1980).
- [64] C.-P. Sun, High-order quantum adiabatic approximation and Berry's phase factor, *J. Phys. A: Math. Gen.* **21**, 1595 (1988).
- [65] G. Rigolin, G. Ortiz, and V. H. Ponce, Beyond the quantum adiabatic approximation: Adiabatic perturbation theory, *Phys. Rev. A* **78**, 052508 (2008).
- [66] J.-F. Chen, C.-P. Sun, and H. Dong, Achieve higher efficiency at maximum power with finite-time quantum Otto cycle, *Phys. Rev. E* **100**, 062140 (2019).
- [67] J.-F. Chen, C.-P. Sun, and H. Dong, Boosting the performance of quantum Otto heat engines, *Phys. Rev. E* **100**, 032144 (2019).
- [68] Y. Sun and H. Metcalf, Nonadiabaticity in stimulated Raman adiabatic passage, *Phys. Rev. A* **90**, 033408 (2014).
- [69] N. V. Vitanov and S. Stenholm, Analytic properties and effective two-level problems in stimulated Raman adiabatic passage, *Phys. Rev. A* **55**, 648 (1997).
- [70] S. Oh, Y.-P. Shim, J. Fei, M. Friesen, and X. Hu, Resonant adiabatic passage with three qubits, *Phys. Rev. A* **87**, 022332 (2013).
- [71] M. Fushitani, C.-N. Liu, A. Matsuda, T. Endo, Y. Toida, M. Nagasono, T. Togashi, M. Yabashi, T. Ishikawa, Y. Hikosaka, T. Morishita, and A. Hishikawa, Femtosecond two-photon Rabi oscillations in excited He driven by ultrashort intense laser fields, *Nature Photon.* **10**, 102 (2016).
- [72] K. Jacobs, *Stochastic Processes for Physicists: Understanding Noisy Systems* (Cambridge University, Cambridge, 2010).